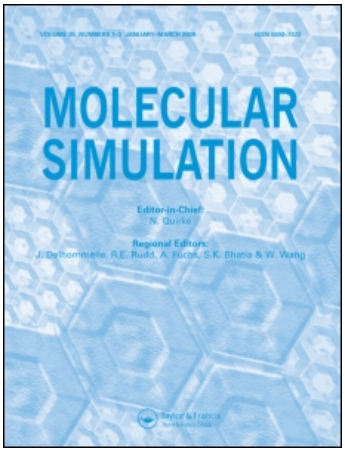

Molecular Simulation
Publication details, including instructions for authors and subscription information:
http://www.informaworld.com/smpp/title~content=t713644482

Dendrimers as Functional Materials. A Molecular Simulation Study of Poly(propylene) Imine Starburst Molecules

Erica Blasizza[a]; Maurizio Fermeglia[a]; Sabrina Pricl[a]
[a] Computer-aided Systems Laboratory, Department of Chemical, Environmental and Raw Materials Engineering - DICAMP, University of Trieste, Trieste, Italy

To cite this Article Blasizza, Erica , Fermeglia, Maurizio and Pricl, Sabrina(2000) 'Dendrimers as Functional Materials. A Molecular Simulation Study of Poly(propylene) Imine Starburst Molecules', Molecular Simulation, 24: 1, 167 — 189
To link to this Article: DOI: 10.1080/08927020008024194
URL: http://dx.doi.org/10.1080/08927020008024194

Molecular Simulation, 2000, Vol. 24, pp. 167–189
Reprints available directly from the publisher
Photocopying permitted by license only

DENDRIMERS AS FUNCTIONAL MATERIALS. A MOLECULAR SIMULATION STUDY OF POLY(PROPYLENE) IMINE STARBURST MOLECULES

ERICA BLASIZZA, MAURIZIO FERMEGLIA
and SABRINA PRICL*

Computer-aided Systems Laboratory, Department of Chemical, Environmental and Raw Materials Engineering - DICAMP, University of Trieste, Piazzale Europa 1, I-34127 Trieste, Italy

(Received April 1999; accepted May 1999)

Dendritic macromolecules are hyperbranched polymers that emanate from a central core, have a defined number of generations and functional end groups, and are synthesized in a stepwise process by a repetitive reaction sequence. This hyperbranched topology results in a unique series of physical and chemical properties exhibited by these molecules which, in turn, could be exploited in a number of diverse possible applications, such as nanoscale catalysis, micelle mimics, immuno-diagnostic and NMR imaging agents, chemical sensors, molecular antennae, just to name a few.

Nonetheless, if on one hand the synthesis procedure allows for control over parameters such as size, shape and reactivity (and hence, on final properties), on the other hand it really hampers the production of large quantities of these materials. Accordingly, their cost is still quite high and, therefore, the materials available for characterization is still rather limited.

Since, however, their full application potentials (particularly in material science and engineering) will not be realized before the understanding of their physical properties is considerably more advanced, in this work we report the results obtained on structural details and related properties of several amine- and nitrile-terminated poly(propylene)imine dendrimer generations by computer simulation studies and discuss them in the light of (scarce) available experimental data.

Keywords: Dendrimers; functional materials; poly(propylene)imine

*Corresponding author.

INTRODUCTION

As a new class of materials, dendrimers (or *starburst polymers*) have recently awakened great interest in the scientific community. Despite the substantial difficulties encountered in their synthesis, a wide range of these substances have been produced and, although only in part, characterized [1].

Starburst dendrimers possess three major architectural components: an initiator core, an interior and an exterior (see Fig. 1). By definition or construction, these three components are interdependent and reflect a unique molecular genealogy. As we progress from the initiator core to an advanced dendrimer stage (or *generation*), this molecular genealogy manifests itself in a variety of ways. Just as we can trace ancestry and lineage in higher organisms, so one can observe a molecular-level parallel by thinking of these transformations in the context of

- stored molecular information at each dendrimer stage;

and

- molecular information transferred to the progeny dendrimer surface at each transformation.

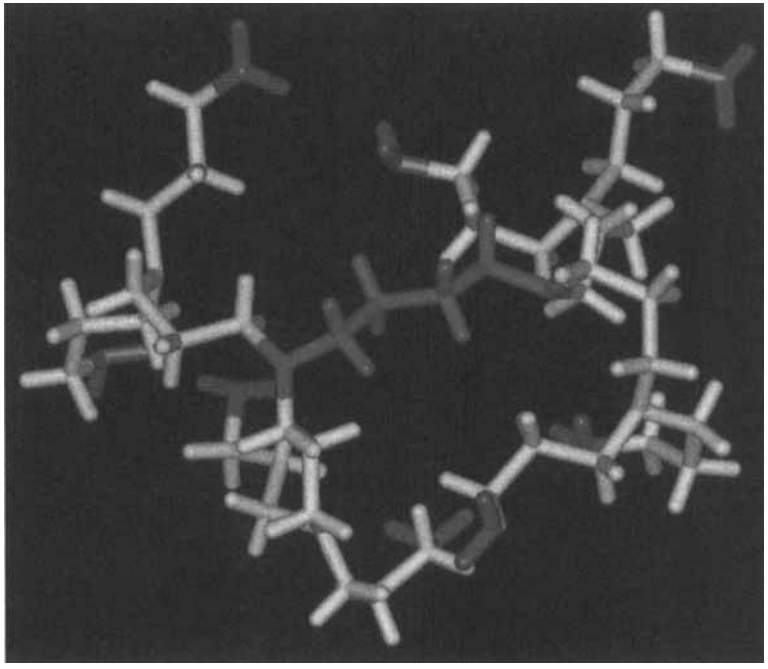

FIGURE 1 Blasizza, Pricl and Fermeglia. (See Color Plate VIII).

Thus, beginning with the core, molecular details are sequentially transcribed and stored to produce interior and, ultimately, exterior features which are characteristic of that dendrimer family. A liaison with some kind of primitive abiotic gene is then quite evident. In this fashion, interior features such as size, chemical composition, flexibility and topology are developed and manifested as stored molecular information. The interior of a dendrimer consists of a scaffolding upon which surface properties such as shape, reactivity, stoichiometry, congestion, special kinetic features, flexibility and *fractal* character can be generated and controlled. These surface features may reflect in several interesting attributes, such as divergent recognition [2] and exo-reception properties [3], which find an analogy in biological processes like, for instance, antibody-antigen recognition [4] and protein–protein interactions [5].

These are by no means the only fascinating aspects of these molecules. In fact, many other potential applications spring from their unusual architecture, which include nanoscale catalysis and reaction vessels, micelle mimics, magnetic imaging agents, immuno-diagnostics, agents for controlled drug delivery, chemical sensors, information-processing materials, high-performance polymers, adhesive and coatings, separation media and molecular antennae for adsorbing light energy and funneling it to a central core (as occur in photosynthetic systems).

Among the plethora of possible dendrimers, poly(propylene)imines have been synthesized on a relatively large scale only in recent years [6, 7]. The synthesis of a poly(propylene) imine dendrimer usually starts with a 1,4-diaminobutane core (DAB), to which four molecules of acrylonitrile are added in a fourfold Michael addition. The resulting tetranitrile of the first generation is then hydrogenated using a transition metal catalyst, which gives the tetra-amine of the first generation. The cycle of Michael additions and hydrogenations is then repeated to obtain higher generations (see Fig. 2).

The potential applications of the poly(propylene)imine dendrimers are generally based on one or more of the following characteristics:

- regular size and shape;
- large number of readily accessible end groups, either nitrile or amine;
- possibility of end group modification in order to tailor properties as solubility, reactivity, toxicity, stability and glass transition temperature;
- polyelectrolyte character;
- possibility of encapsulating guest molecules.

Since, however, their full application potentials (particularly in materials science and engineering) will not be realized before the understanding of their physical properties is considerably more advanced, in this work we

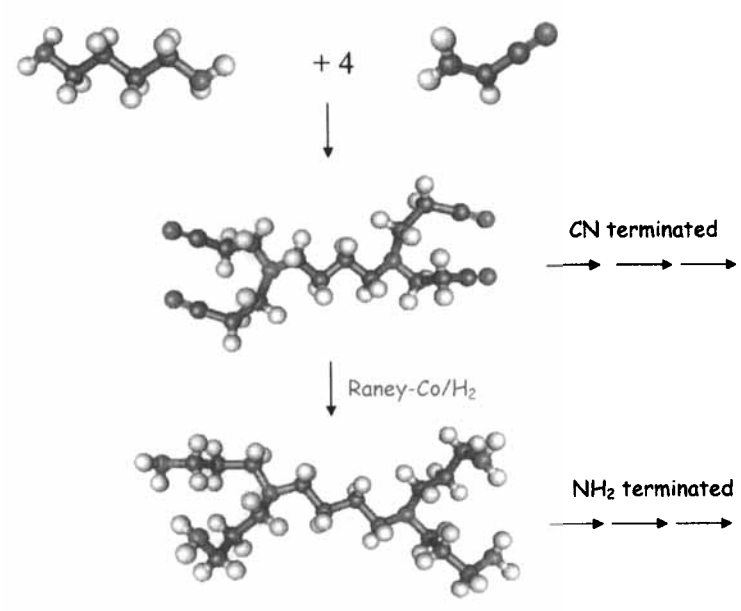

FIGURE 2 Blasizza, Pricl and Fermeglia. (See Color Plate IX).

report the first results obtained on structural details and related physical properties of several poly(propylene imine) dendrimer generations (both amine- and nitrile-terminated, hereafter indicated by DAB-NH_2 and DAB-CN, respectively) by computer simulation studies.

COMPUTATIONAL DETAILS

All simulations were run on a Silicon Graphics Origin 200 (microprocessor MIPS RISC 10000, 64 bit CPU, 128 MB RAM) and performed by using the commercial software *Cerius*[2] (v. 3.8) from Molecular Simulation Inc. (for both MM and MD simulations). The generation of accurate model structures of both dendrimer series was conducted as follows. For each dendrimer, the molecule was built and its geometry optimized *via* energy minimization using the DREIDING 2.1 force field [9]. The DREIDING FF belongs to the general class of force fields, and has been proved to yield sufficiently accurate structures for organic molecules. Although we could have used more accurate FFs, the main reason for our choice relies on the fact that it is a commercial FF having an explicit term for the hydrogen-bond energy component, which allowed us to determine the corresponding component of the solubility product δ, as described below.

The molecules were modeled to have a total charge equal to zero, and the distribution of the partial charge within each molecule was determined by the charge equilibration method of Rappé *et al.* [9]. Energy was minimized by up to 5000 Newton–Raphson iterations. Following this procedure, the root-mean-square (rms) atomic derivatives in the low energy regions were smaller than 0.05 kcal/mole Å. Long-range nonbonded interactions were treated by applying suitable cutoff distances, and to avoid the discontinuities caused by direct cutoffs, the cubic spline switching method was used. van der Waals distances and energy parameters for nonbonded interactions between heteronuclear atoms were obtained by the 6th-power combination rule proposed by Waldman and Hagler [10].

The calculation of molecular surfaces was performed using the so-called Connolly dot surfaces algorithm [11, 12]. Accordingly, a probe sphere of a given radius, representing the solvent molecule, is placed tangent to the atoms of the molecule at thousands different positions. For each position in which the probe does not experience van der Waals overlap with the atoms of the molecule, points lying on the inward-facing surface of the probe sphere become part of the molecule solvent-accessible surface. According to this procedure, the molecular surface generated consists of the van der Waals surface of the atoms which can be touched by a solvent-sized probe sphere (thus called contact surface), connected by a network of concave and saddle surfaces (globally called reentrant surface), that smoothes over crevices and pits between the atoms of the molecule. The sum of the contact and the reentrant surface form the so-called molecular surface (MS); this surface is the boundary of the molecular volume (MV) that the solvent probe is excluded from if it is not to undergo overlaps with the molecule atoms, which therefore is also called solvent-excluded volume. Finally, performing the same procedure by setting the probe sphere radius equal to zero, the algorithm yields the van der Waals surface (WS).

The details of the isolated molecular structures at 298 K were obtained by performing MD simulations both under NVT and NVE conditions. For the calculation of the thermophysical properties of the dendrimers, a suitable number of molecules were confined in a cubic box with periodic boundary conditions (PBC); the maximum number of molecules was 256 for DAB-NH_2 and DAB-CN, so that the total number of atoms in the periodic cell was 4608 for DAB-NH_2 and 4096 for DAB-CN, respectively. For all successive generation, the number of molecules in the simulations boxes was rescaled in order to maintain the total number of atoms approximately constant. In order to minimize the artifact of periodicity, a cutoff distance was set equal to half the box length. The

resultant structures were relaxed *via* MM, again using the DREIDING FF; in this case, the Ewald technique was employed in handling nonbonded interactions.

Such a straightforward molecular mechanics scheme is likely to trap the simulated system in metastable local high-energy minima. To prevent the system from such entrapments, the relaxed structures were subjected simulated annealing (5 repeated cycles from 298 K to 1000 K and back) using constant volume/constant temperature (NVT) MD conditions. At the end of each annealing cycle, the structures were again relaxed *via* FF, using a rms force less than 0.1 kcal/mole Å for the molecule and 0.1 kcal/mole $Å^3$ for the stresses on the periodic boxes as convergence criteria. Both convergence criteria were simultaneously satisfied for the system to be relaxed completely. The simulation box was allowed to vary in size and shape during energy minimization, in order to find the equilibrium density for each structure.

Each molecular dynamics run was started by assigning initial velocity for the atoms according to a Boltzmann distribution at $2 \times T$. Temperature was controlled *via* weak coupling to a temperature bath [13], with coupling constant $\tau_T = 0.01$ ps, whereas pressure was kept constant by coupling to a pressure bath [14], with relaxation time $\tau_P = 0.1$ ps. The Newton molecular equations of motion were solved by the Verlet leap-frog algorithm, using an integration step of 1 fs. Since the partial charges assigned by the charge equilibration method are dependent on structure geometry, they were updated regularly every 100 MD steps during the entire MD runs.

Each MD simulation consisted in a system equilibration phase, during which the equilibration process was followed by monitoring the behavior of both kinetic and potential energy and the time evolution of density, and a successive data collection phase. Almost in all cases, the energy components as well as density have ceased to show a systematic drift and have started to oscillate about steady mean values around 30 ps. Accordingly, equilibration phases longer than 100 ps (*i.e.*, 1000,000 MD steps with time step = 1 fs) and data acquisition runs longer than 400 ps were judged not necessary to enhance data accuracy.

RESULTS AND DISCUSSION

Figures 3(a) and (b) show the wireframe structures of generation 0 through 4 for DAB-NH_2 and DAB-CN dendrimers obtained as a result of the first

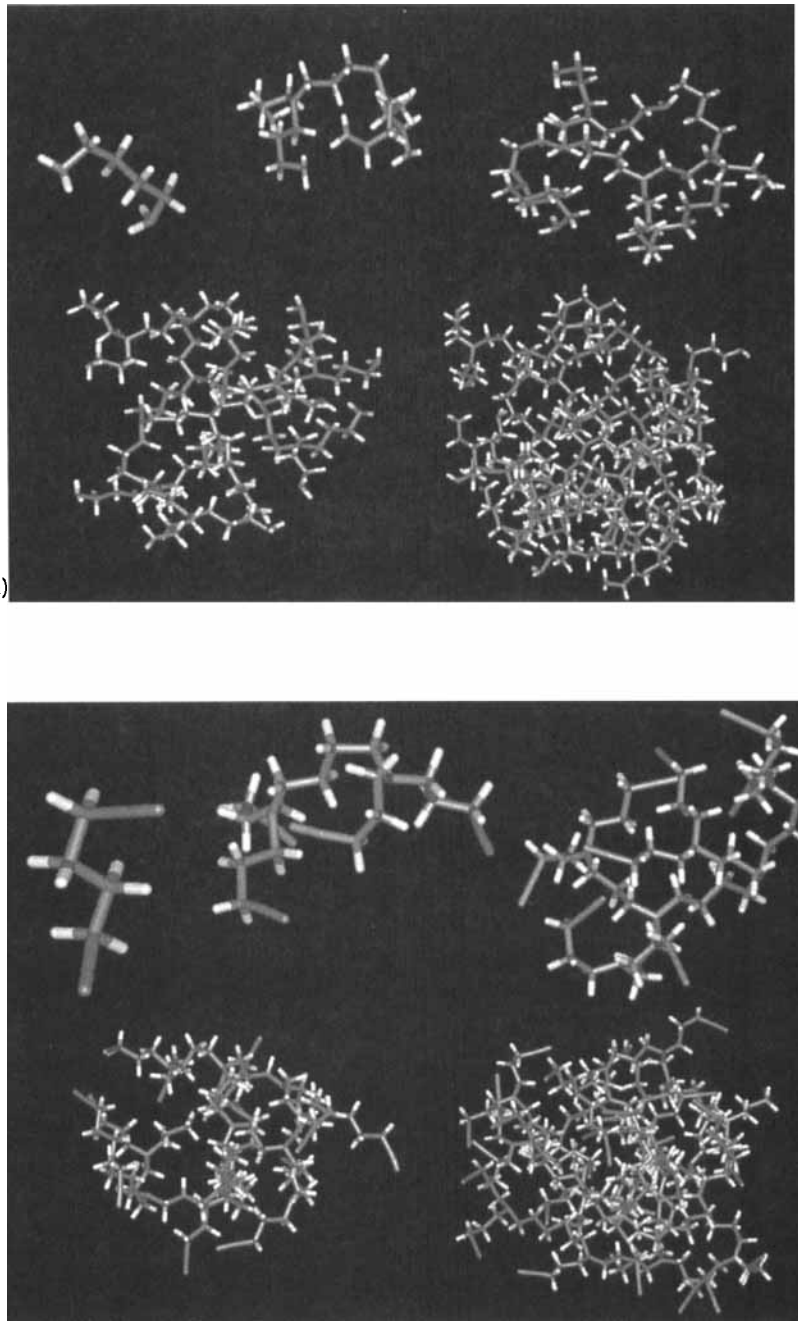

FIGURE 3

structural investigations performed with MD simulations under NVT and NVE conditions. If the first generations are quite open, by generation 2 the dendrimers have already reached the conformation of a tangled mass. A clearer illustration of the corresponding structures is presented in Figures 4(a) and (b) by means of the Connolly dot surface algorithm. The early generations are somewhat amorphous in shape but the second ones are already clearly spherical. This transition to a spheroidal form can be quantified by the aspect ratio of the principal moments for various generations (see Figs. 5(a) and (b)). The aspect ratios decrease from 2.5 and 2.0 to 1.0 and even less for DAB-NH_2 and DAB-CN, respectively. In the case of DAB-NH_2, the high *initiator core multiplicity* ($N_c = 4$), combined with the \û*branch multiplicity* ($N_b = 2$) results in very compact, highly congestemicrodomains which possess, at most, only very small internal voids. Quite analogous results are shown by its parent molecule DAB-CN. A quantitative analysis of the internal surface area and solvent filled volume can be made by resorting to the concept of solvent contact surface as determined by the Connolly algorithm. Figure 6 contains plots of *CS* as a function of the probe radius p_r for various DAB-NH_2 and DAB-CN

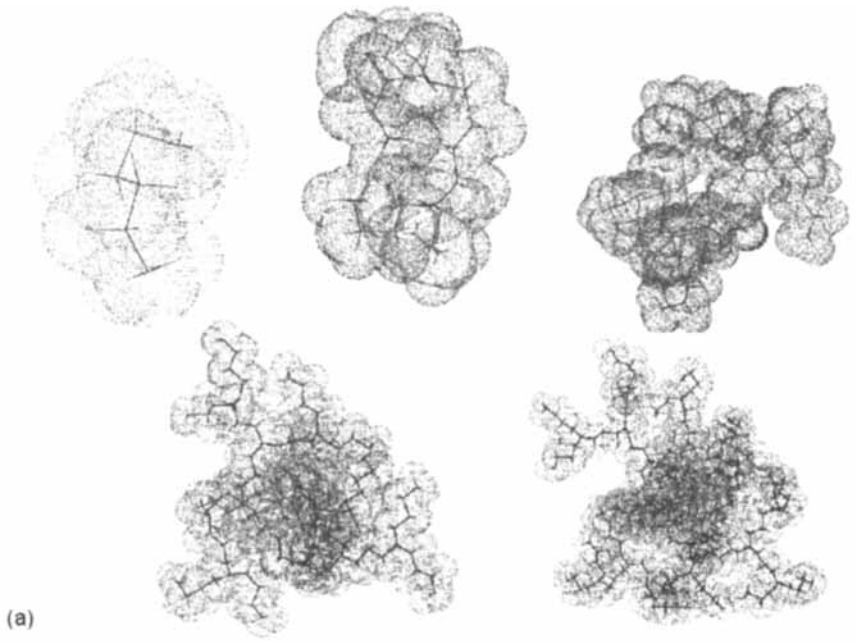

FIGURE 4

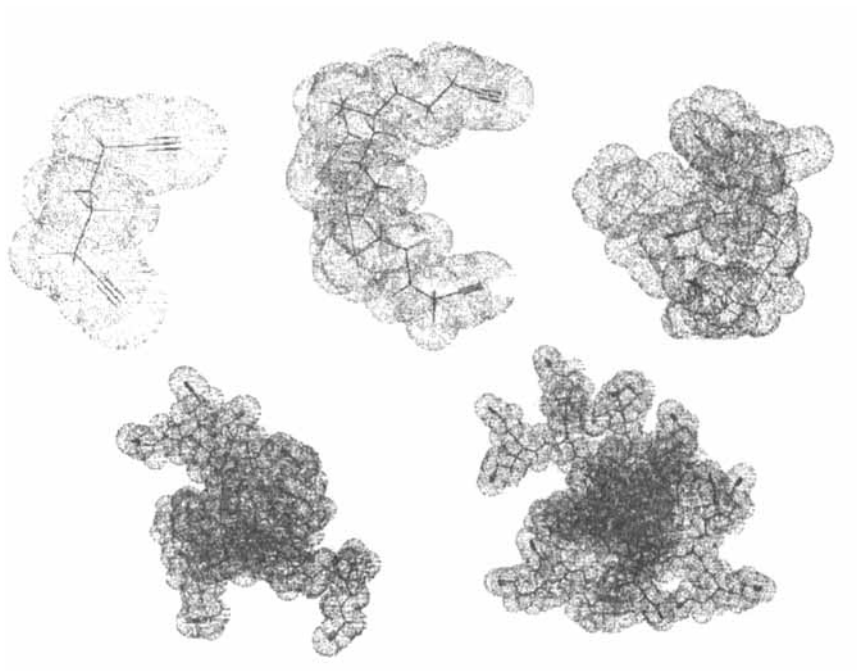

(b)

FIGURE 4 (Continued).

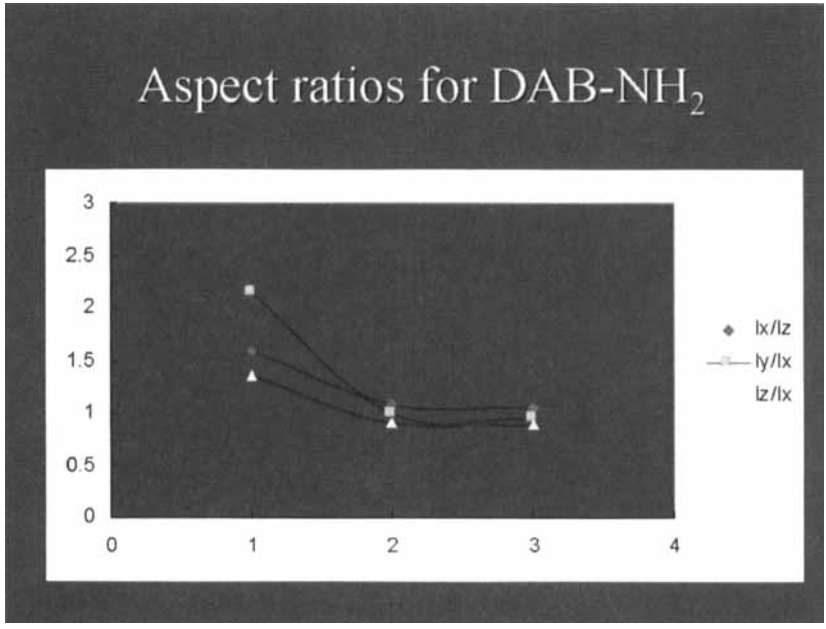

(a)

FIGURE 5

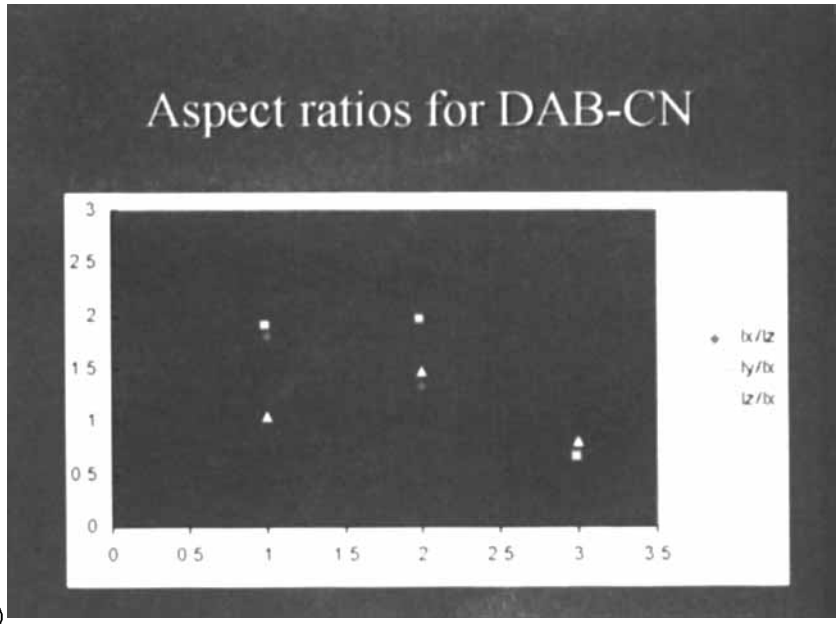

(b)

FIGURE 5 (Continued).

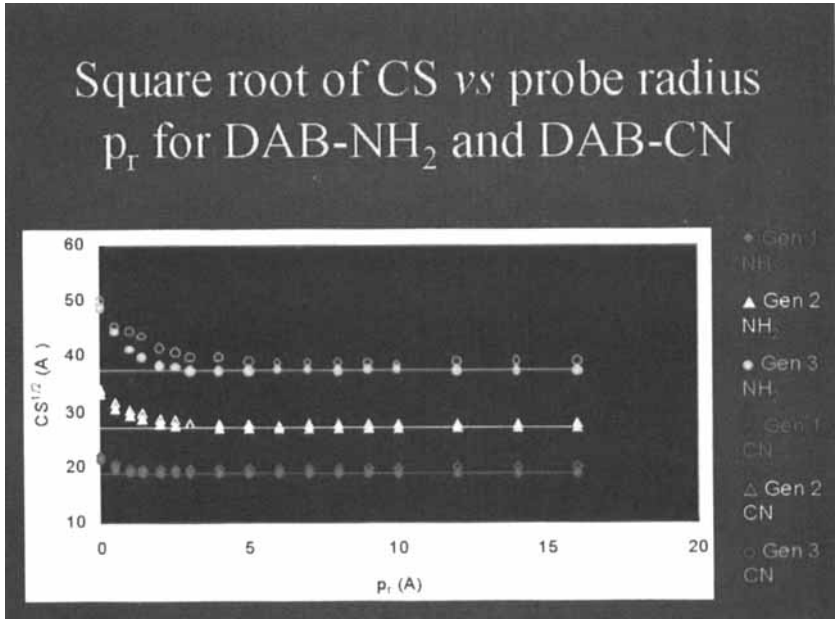

FIGURE 6

simulated. Indeed, for large values of p_r, CS becomes independent of p_r, as expected; nevertheless, for small probe radii, a deviation from linearity is observed, owing to the extra surface area associated with the interior regions of the molecule. A linear regression analysis (shown in Fig. 6 only for DAB-NH_2 for the sake of readability) of these data indicates both the amount of any internal surface area (A_{INT}) and the size ($R_{A_{INT}}$) of the dendrimer (see Tab. I). As we can see, again for both DAB-NH_2 and DAB-CN, the internal surface area A_{INT} increases from approximately 4% for generation 1 to 19% for generation 3. This behavior is utterly similar to that exhibited by another series of dendrimers characterized by the same multiplicity, the so-called polyether dendrimers, for which A_{INT} ranges from 1% at generation one to 20% at generation 3 and 4 [1].

A measure of the volume associated with the internal cavities of the DAB dendrimers can be achieved analyzing the behavior of the solvent excluded volume V_{SE} again as a function of the probe radius p_r. If we consider Figure 7, where we report $V_{SE}^{1/3}$ *vs.* p_r, we see that again a linear relationship is obtained for large probe radii but there is a limited deficit of volume for small p_r (V_{INT}) (from 5% to 15% for both dendrimer series, see Tab. I), owing to the presence of small internal cavities and channels. Once again, this behavior is reminiscent of that shown by polyether starburst molecules [1].

Molecular modeling and molecular dynamics simulations were also used to estimate the size of both series of DAB dendrimers as a function of generation (see Tab. I). Five quantities were calculated from these experiments:

TABLE I

	A_{INT} (%)	R_{A_INT} (Å)	V_{INT} (%)	$R_{V_{INT}}$ (Å)	R_{gNVT} (Å)	R_{gNVE} (Å)	R_{CKP} (Å)
Gen NH_2							
0					2.28	2.21	2.3
1	4.1	5.3	8.7	4.8	4.05	4.08	4.0
2	9.0	7.6	12	6.7	6.01	6.58	7.8
3	18	10	14	8.9	7.77	7.62	10
Gen CN							
0					2.40	2.38	2.4
1	4.4	5.5	5.3	4.7	4.42	4.49	4.5
2	9.4	7.8	12	6.8	6.09	6.79	7.4
3	19	11	15	9.1	7.59	7.56	11

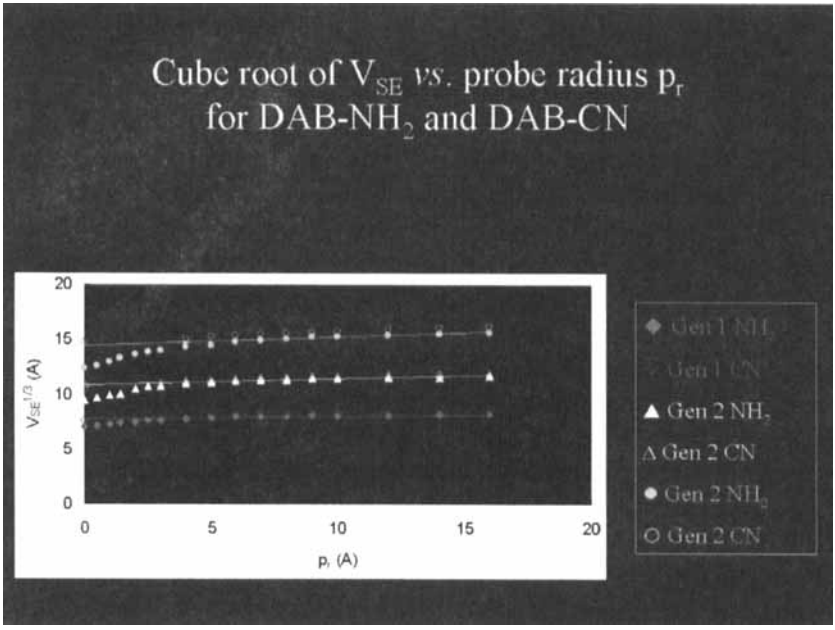

FIGURE 7

- $R_{A_{INT}}$, the molecular radius determined from the linear regression fits of $CS^{1/2}$ *vs.* p_r;
- $R_{V_{INT}}$, the molecular radius determined from the linear regression fits of $V_{SE}^{1/3}$ *vs.* p_r;
- R_{gNVT}, the molecular value of the radius of gyration, averaged over the entire set of trajectories during the collection phase of an NVT experiment (from 100 to 500 ps);
- R_{gNVE}, the value of the radius of gyration, averaged over the entire set of trajectories during the collection phase of an NVE experiment (from 100 to 500 ps);
- R_{CKP}, the maximal end-to-end distance between terminal heteroatoms (N in both cases), determined periodically and averaged over the entire set of NVT trajectories.

All values are plotted together in Figure 8(a) for DAB-NH_2 and in Figure 8(b) for DAB-CN. Generally speaking, there is a very good agreement between all series of calculated values; furthermore, the agreement with the experimentally available radius of gyration values [6] is indeed extremely good (see Figs. 8(c), (d)).

A closer inspection of Figures 8 reveals that, for both series of dendrimers, the molecular dimensions, as expressed by R_g, increase in a

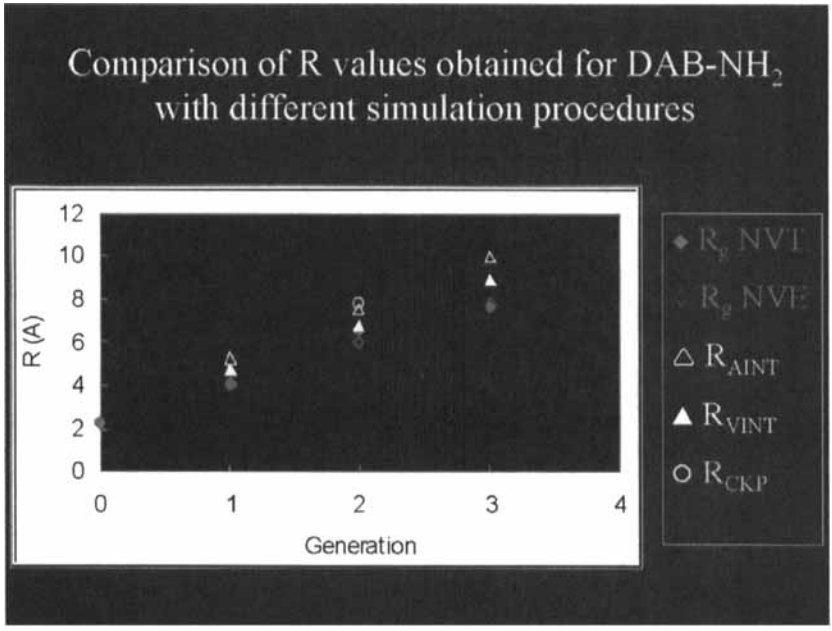

(a)

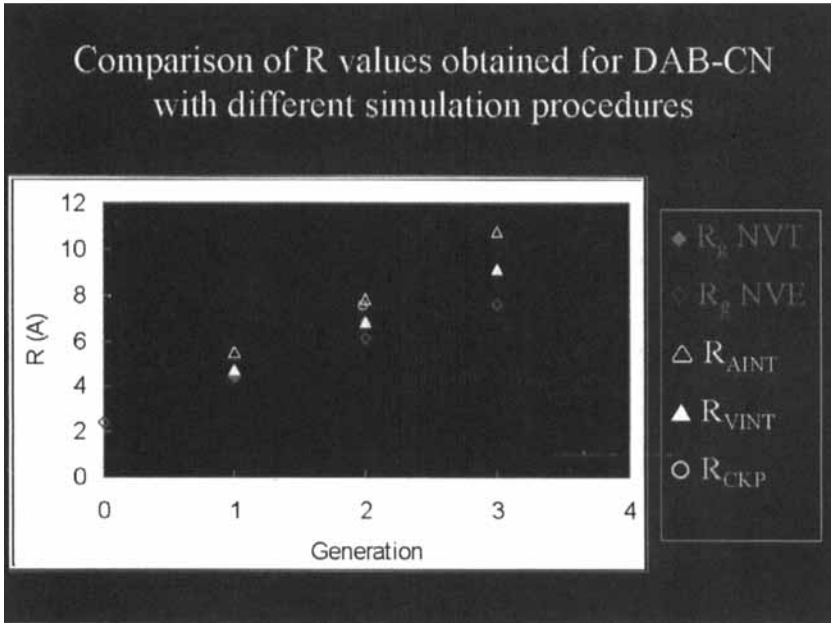

(b)

FIGURE 8

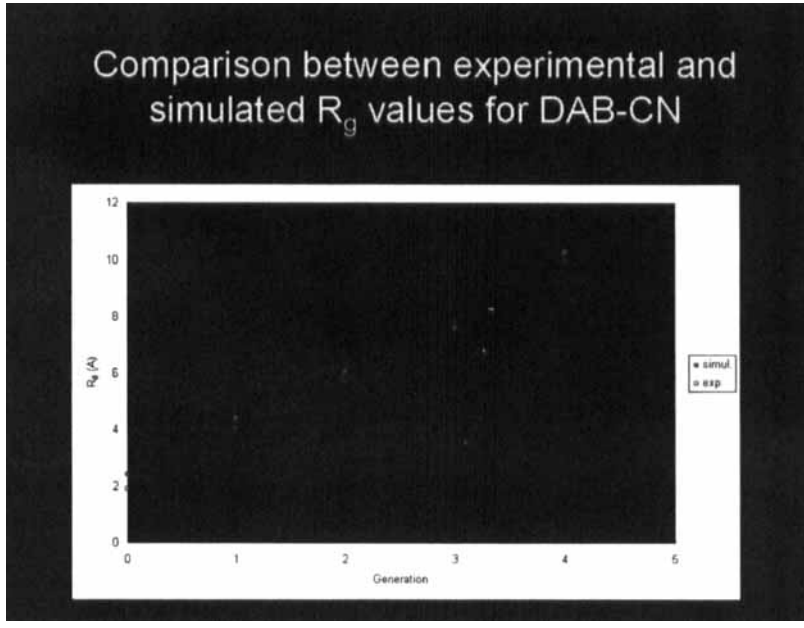

(c)

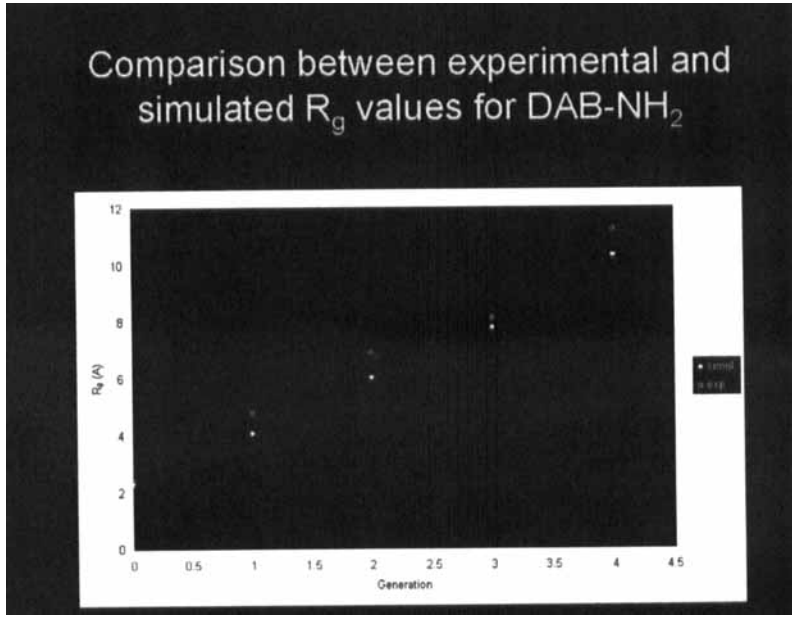

(d)

FIGURE 8 (Continued).

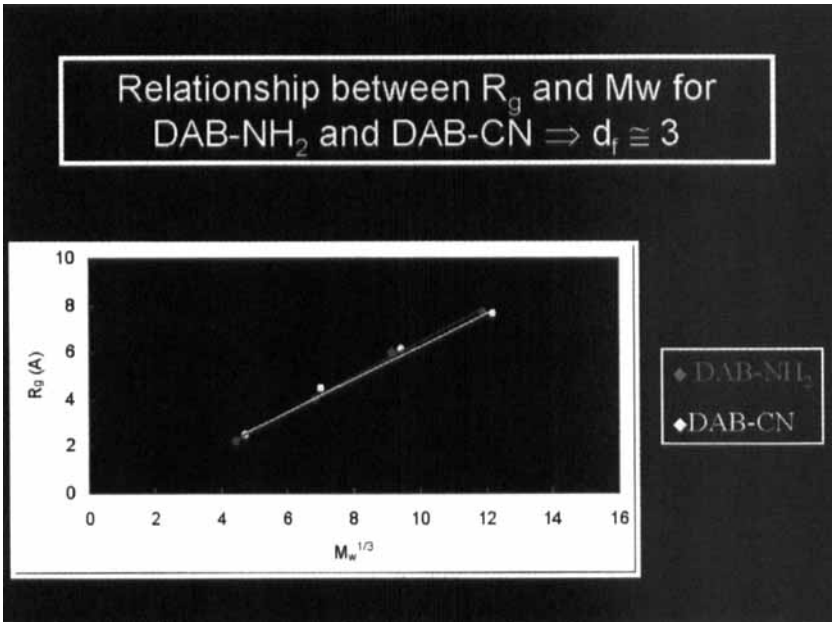

FIGURE 9

linear fashion with the generation number. Moreover, the radius has a linear relation with the molecular weight (see Fig. 9), which is a further indication for a compact space filling structure with *fractal dimensionality* d_f of about 3. Once again, the results obtained from our simulations are in agreement with the only available experimental results [6].

As mentioned earlier, parameters such as size, shape and multiplicity are transcribed, and displayed throughout the dendrimer development. These variables can have dramatic effects on the ultimate shape, the interior topology and the exterior surface properties (alias congestion) of the developing dendrimer. Mathematically, we can appraise dendrimer surface congestion as a function of generation from the following relationship:

$$A_Z = A_D/N_Z \propto R^2/N_c N_b^G$$

in which A_Z is the surface area per terminal group Z, A_D is the dendrimer surface area and N_Z is the number of terminal groups Z per generation. From this relation we can see that at higher generations G, the surface area per Z group should become increasingly smaller and experimentally approach the cross sectional area of the van der Waals dimensions of the

surface group Z. The generation G thus reached is referred to as the *starburst dense-packed generation*. As predicted by de Gennes and Hervet [15], ideal starburst growth without branch defects is possible only for those generations preceding the dense-packed state. This critical dendrimer property gives rise to self-limiting starburst dimensions, which are a function of the branch-segment length l, the core multiplicity N_c, the branch-juncture multiplicity N_b and the steric dimensions of the terminal group Z. Since the dendrimer radius in the expression above is dependent of l, larger l values will delay this congestion, whereas larger N_c and N_b values and large Z dimensions will dramatically hasten it.

Computer-assisted molecular simulations allowed us to determine the surface area per Z group, A_Z, as a function of generation (see Fig. 10). In both cases, the curves show that A_Z slowly increase for generations 0–3 and then seems to reach a plateau with generation 4. Very likely, with generation 5, it will begin to decline, presumably owing to surface congestion. Additional physical evidence that support the development of congestion as a function of generation can be found in the behavior of density *vs.* dendrimer generation obtained from molecular dynamics simulations under both NPT and NPH conditions (see Fig. 11): the density

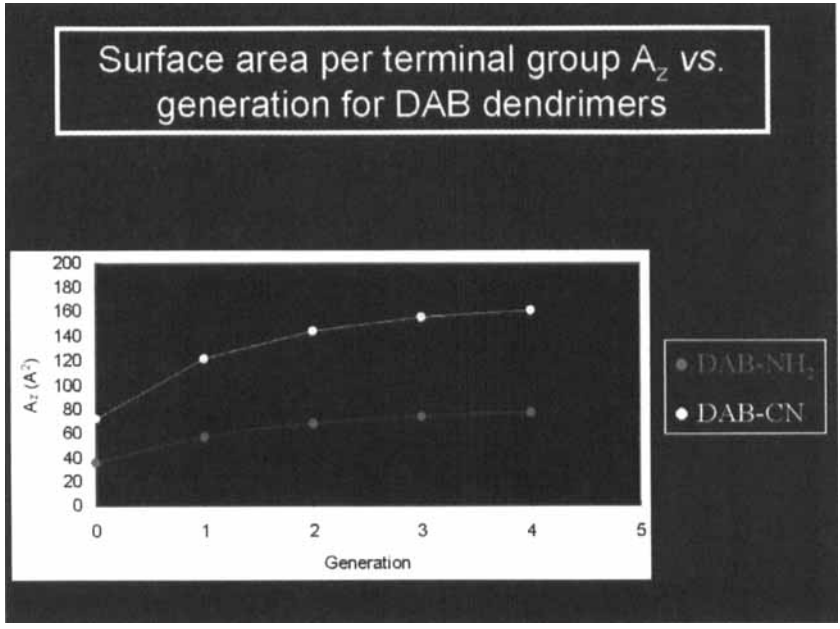

FIGURE 10

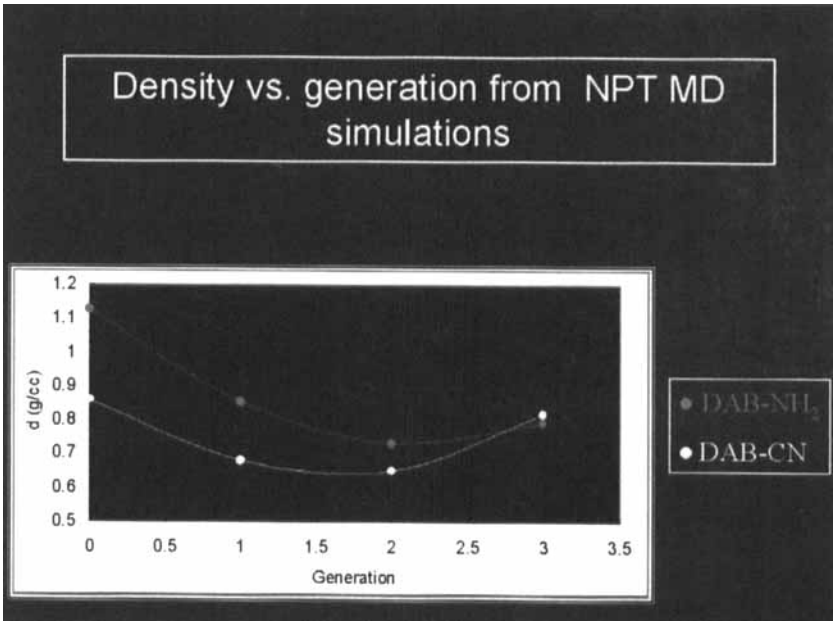

FIGURE 11

clearly minimizes between generation 2 and 3, and then begins to increase owing to the increasingly larger exponential accumulation of surface groups as a function of generation. This set of evidences match that exhibited by another series of dendrimers, the poly(amido amine) molecules or PAMAM dendrimers [1]. Obviously, further work is necessary (and is currently in progress) on further generations in order to quantify the dense-packed generation for these series of DAB dendrimers.

Molecular dynamics simulations under different ensembles allowed us to characterize some thermophysical properties of DAB-based dendrimers, of which very little is known, if at all. A quantity of practical interest, which can be easily obtained from such virtual experiments, is the *solubility product* δ and its three components δ_d, δ_p and δ_{hb}, respectively [16]. Table II reports the values of the solubility product and its components for the DAB-NH_2 series at 298 K, obtained according to the following procedure.

By definition, the solubility product δ is the square root of the cohesive energy density e_{coh} which, in general, is defined as the ratio of the cohesive energy E_{coh} and the molar volume V at a given temperature. E_{coh}, in turn, is defined as the increase in internal energy per mole of substance if all intermolecular forces are eliminated. In our simulated systems, each

TABLE II

DAB-NH_2 Generation	$\delta(J/cc)^{1/2}$	$\delta_d(J/cc)^{1/2}$	$\delta_p(J/cc)^{1/2}$	$\delta_{hb}(J/cc)^{1/2}$	*EDA* $\delta(J/cc)^{1/2}$	*DAB-NH_2* $\gamma(dyne/cm)$	*EDA* $\gamma(dyne/cm)$
0	21.7	14.7	13.2	9.04	25.2	42.29	40.77
1	18.1	12.5	10.1	8.22		42.67	
2	15.8	11.7	8.95	5.82		43.89	
3	17.4	13.4	5.26	9.80		70.24	
DAB-CN Generation	$\delta(J/cc)^{1/2}$	$\gamma(dyne/cm)$					
0	24.1	58.49					
1	21.1	62.21					
2	18.2	66.45					
3	19.9	96.50					

molecule is surrounded by other molecules that are simply displaced images of the molecule itself. The cohesive energy is the energy of interactions between these images. Accordingly, the values of can be obtained from simulation by calculating the difference between the nonbonded energy of the periodic structure and the corresponding value of E_{nb} for an isolated molecule *in vacuum* at the same temperature.

In all our cases, a comparison between the energy components of the isolated and of the bulk molecules reveals that the valence contribution to E_{tot} is nearly the same for both systems, and the major difference is indeed given by the nonbonded term $E_{nb} = E_{vdw} + E_{coul} + E_{hb}$. Actually, it can be easily understood that the reduction in the total energy for the molecule in bulk rises solely due to the intermolecular nonbonded attractive interactions between the atoms from neighboring molecules.

For DAB-CN, since the intermolecular hydrogen-bonding term of the forcefield is correctly predicted to be equal to zero, the evaluation of the δ components is impossible; accordingly, in Table II we report only the value of the total solubility product for this dendrimer series. The behavior of δ *vs.* generation, graphically illustrated in Figure 12, seems quite

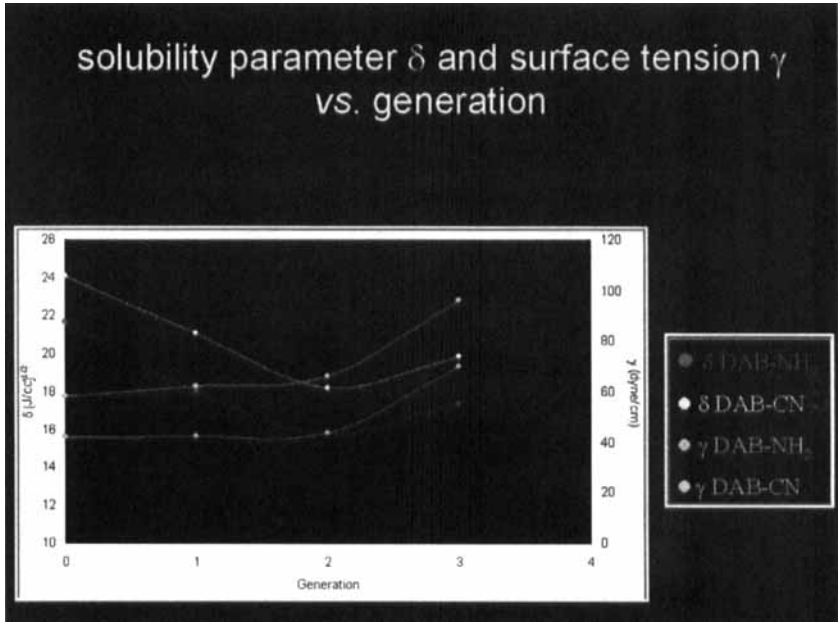

FIGURE 12

reasonable. The relevant experimental values are not available but the comparison of the values of the first member of the DAB-NH_2 series (1,4-diaminobutane) with its shorter analogue (ethylene diamine, EDA) seems rather comforting (see Tab. II). For DAB-CN, no data are available on any shorter analogue, but the value for a close compound, butanenitrile ($\delta = 20.5\,J^{1/2}/cc^{3/2}$) indicates that the simulated value can be considered realistic. The higher δ values obtained for the DAB-CN dendrimer series are justified by the higher polar contribution of the CN group with respect to the amino group.

Strictly related to the solubility product is another thermophysical property, whose importance in chemical engineering is increasing steadily: the surface tension γ. This quantity can be calculated from δ according to the following relationship [17]:

$$\gamma = [(\delta \times (V)^{1/3})^{0.43}/4.1]^{1/0.43}$$

and the corresponding values are reported numerically in Table II and graphically in Figure 12. As we can see, between generations 2 and 3 there

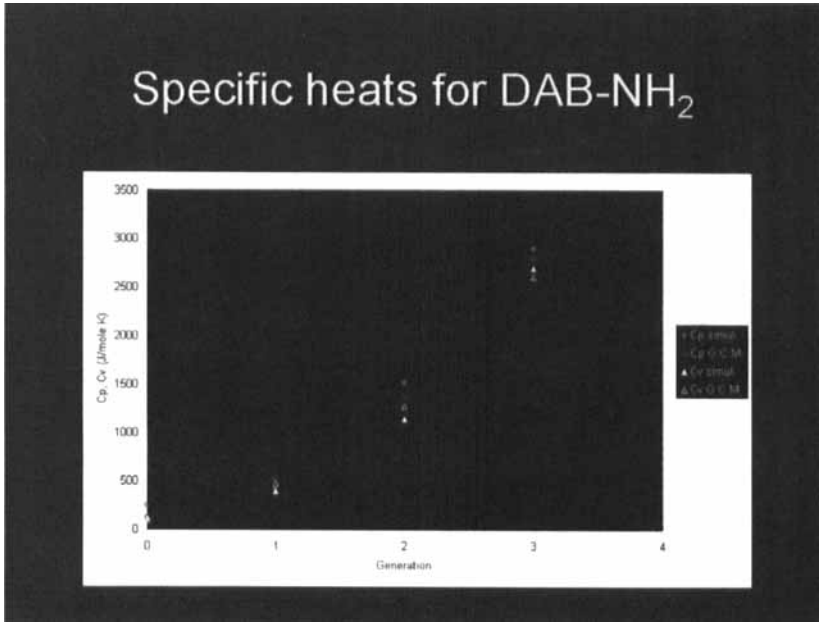

(a)

FIGURE 13

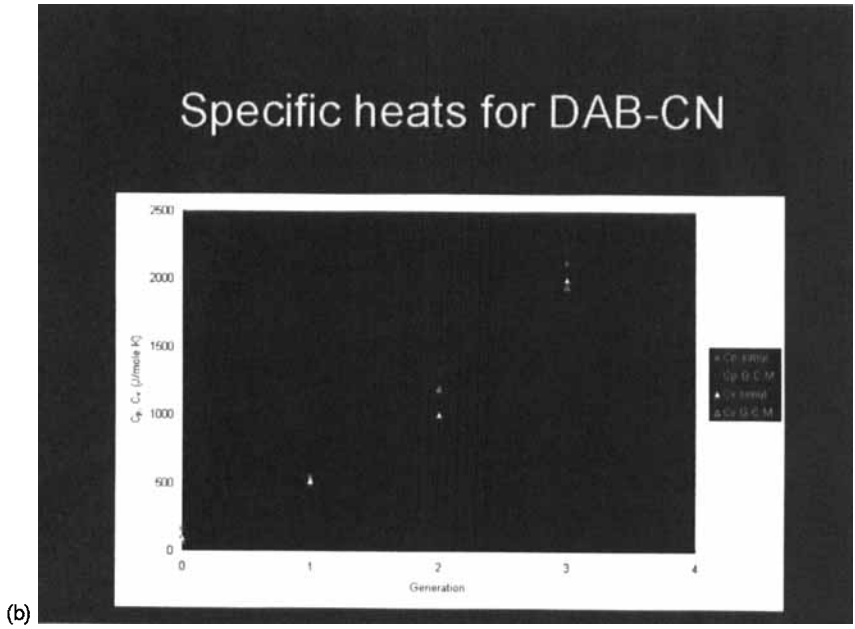

(b)

FIGURE 13 (Continued).

is a rapid increase in the γ values, in harmony with all other evidences for these starburst molecules. The values of γ obtained are consistent with those of most common organic solids and polymers, although those calculated for generation 3 are rather high. Obviously, an interpretation of the latter is not possible at present and data on further generations (in progress) are clearly needed to confirm these evidence.

Another interesting series of data obtained from simulation concern specific heats, isothermal compressibilities and thermal expansion coefficients. The relevant values are reported in Figures 13(a), 13(b), 14 and 15. Since the literature is devoid of data, we performed a very rough check of our results by calculating the values of the corresponding properties by group contribution techniques (G.C.T.) [18, 19]. Although these preliminary results should be considered with care, the fair agreement between simulated and calculated quantities seems to be encouraging. A brief comment appropriate at this stage is again that, for all these quantities, the values obtained from molecular dynamics simulations are in good agreement with those calculated by group contribution methods and are consistent with the available values for organic substances of comparable molecular weight or many organic polymers.

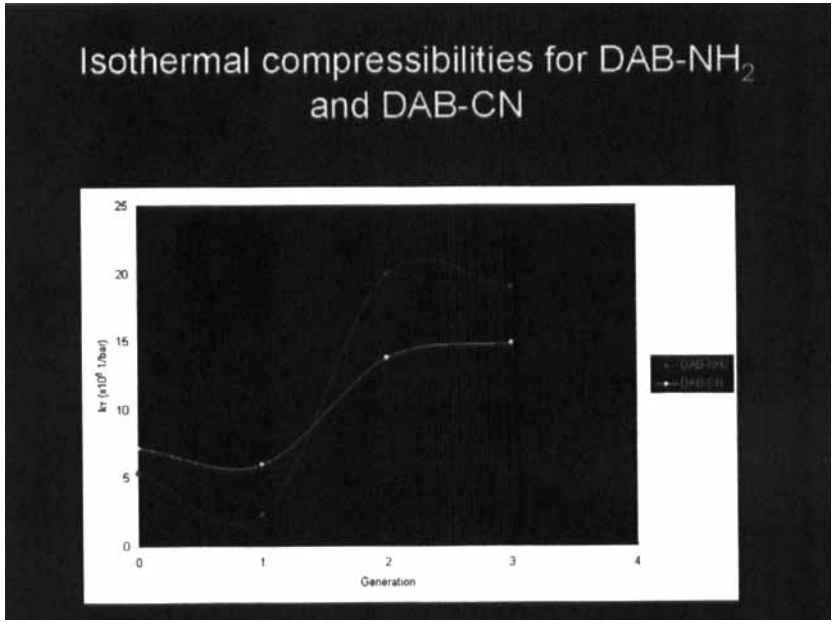

FIGURE 14

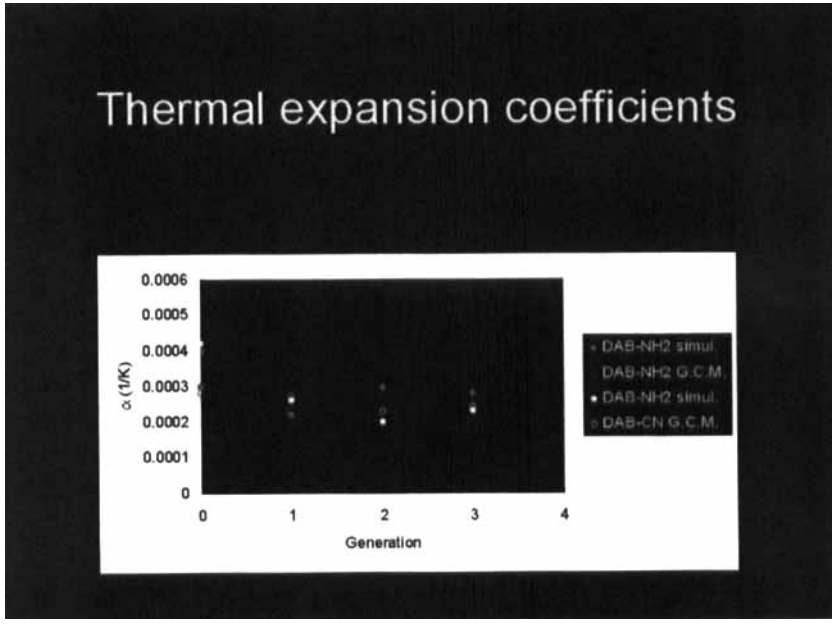

FIGURE 15

CONCLUSIONS AND FUTURE WORK

This paper presents the preliminary results obtained from MM/MD simulations on two series of DAB-based dendrimers. From the structural point of view, the agreement of the results achieved from computer experiments and the relevant experimental observations is very good. The values of the first thermophysical properties obtained from simulations up to date, although no experimental data are available for comparison, seem reasonable and are in accordance both with values calculate from group contribution techniques and with those reported for most common organic substance and polymers. Further work is currently in progress to confirm the results obtained and to expand the data series to higher dendrimer generations.

References

[1] Tomalia, D. A., Naylor, A. M. and Goddard, W. A. (1990). *Angew. Chem. Int. Ed. Engl.*, **29**, 138.
[2] Cram, D. J. and Cram, J. M. (1988). *Angew. Chem. Int. Ed. Engl.*, **27**, 109.
[3] Lehn, J. M. (1988). *Angew. Chem. Int. Ed. Engl.*, **27**, 91.
[4] Amit, A. G., Mariuzza, A. R., Phillips, S. E. V. and Poljak, R. J. (1986). *Science*, **233**, 7047.
[5] Lewis, M. and Rees, D. C. (1985). *Science*, **230**, 1163.
[6] de Brabander, E. M. M. and Meier, E. W. (1993). *Angew. Chem. Int. Ed.*, **32**, 1308.
[7] de Brabander, E. M. M., Brackman, J., Mure-Mak, M., de Man, H., Hogeweg, M., Keulen, J., Scherrenberg, R., Coussens, B., Mengerink, Y. and van der Waal, Sj. (1996). *Macromol. Symp.*, **102**, 9.
[8] Mayo, S. L., Olafson, B. D. and Goddard III, W. A. (1990). *J. Phys. Chem.*, **94**, 8897.
[9] Rappé, A. K. and Goddard III, W. A. (1991). *J. Phys. Chem.*, **95**, 3358.
[10] Waldman, M. and Hagler, A. T. (1993). *J. Comput. Chem.*, **14**, 1077.
[11] Connolly, M. L. (1983). *J. Appl. Crystallogr.*, **16**, 548.
[12] Connolly, M. L. (1985). *J. Am. Chem. Soc.*, **107**, 1118.
[13] Berendsen, H. J. C., Postma, J. P. M., van Gunsteren, W. F., DiNola, A. and Haak, J. R. (1984). *J. Chem. Phys.*, **81**, 3684.
[14] Andersen, H. C. (1980). *J. Chem. Phys.*, **72**, 2384.
[15] de Gennes, P. G. and Hervet, H. J. (1983). *Phys. Lett.*, **44**, 351.
[16] Hansen, C. M. (1969). *Ind. Eng. Chem. Res.*, **8**, 2.
[17] Hildebrand, J. H. and Scott, R. L., *The Solubility of Non-electrolytes*, van Nostrand, princeton, N.J., 1950.
[18] Bondi, A., *Physical Properties of Molecular Crystals, Liquids and Glasses*, John Wiley and Sons, New York, 1968.
[19] van Krevelen, D. W., *Properties of Polymers: Their Correlation with Chemical Structure, Their Numerical Estimation and Prediction from Additive Group Contributions*, Elsevier Science Publishers, Amsterdam, 1990.